

## Conductance of Small Molecular Junctions

N. B. Zhitenev, H. Meng, and Z. Bao

*Bell Laboratories, Lucent Technologies, Murray Hill, New Jersey 07974*

(Received 28 January 2002; published 17 May 2002)

A new method of fabricating small metal-molecule-metal junctions is developed, approaching the single-molecule limit. The conductance of different conjugated molecules in a broad temperature, source-drain, and gate voltage regime is reported. At low temperature, all investigated molecules display sharp conductance steps periodic in source-drain voltage. The position of these steps can be controlled by a gate potential. The spacing corresponds to the energy of the lowest molecular vibrations. These results show that the low-bias conductance of molecules is dominated by resonant tunneling through coupled electronic and vibration levels.

DOI: 10.1103/PhysRevLett.88.226801

PACS numbers: 73.63.-b, 73.23.-b, 73.40.Gk

The research of electronic properties of nanometer scale molecular systems is driven by its potential use for electronic applications. Electronically functional molecular units of sizes much smaller than accessible with modern lithography tools can be synthesized relatively inexpensively and in large quantities. The major challenge on the road to molecular electronics is to organize the molecular building blocks into micro- and eventually macroscopic circuits.

Many different approaches to contact a small number of molecules have been developed in recent years. Some of the methods exploit the flexibility of tunable contacts to molecules afforded by scanning probes [1–3] or break junctions [4,5]. Other methods use a fixed contact arrangement. These include trapping molecules on prefabricated contacts [6,7], depositing small metal contacts on self-assembled molecular monolayers (SAM) in a nanopore geometry [8], or using shadow masks [9,10]. In general, the conductance of a molecule is quite low, in the range of  $10^{-9}$ – $10^{-7} \Omega^{-1}$ . The Fermi level of typical metals falls in the gap between the highest occupied and lowest unoccupied molecular orbitals.

Here we employ a new technique that combines some advantages of both tunable and fixed contacts. The method is based on the fabrication of metal single electron transistors (SETs) on scanning tips [11] that exploits the smallness of the tip geometry with shadow angle evaporation. The approach is extended to fabricating small junctions with molecules inside. The device performance can be monitored during fabrication as with tunable contacts, but the contact geometry is fixed, providing good mechanical and thermal stability. Using this geometry, we have found new reproducible features in the low-bias conductance of molecules.

The fabrication starts by pulling a quartz rod with a square cross section of 1 mm side (Fig. 1a). The typical diameter of the tip is in the 20–30 nm range, as confirmed by analyzing images of local electric field on surfaces of metals or semiconductors acquired with an SET. Metal electrodes are deposited onto different faces

of the tip. The square tip shape helps to avoid shorts, providing good separation between the electrodes. The fabrication sequence is shown in Fig. 1b. The molecular junction is formed during the last deposition step while monitoring the source-drain conductance. The detectable conductance of the order of  $10^{-9} \Omega^{-1}$  appears at the thickness of deposited gold of  $\sim 20$ – $25 \text{ \AA}$ , then grows in jumps reaching the range of  $10^{-7}$ – $10^{-6} \Omega^{-1}$  in 4–5 steps at Au thickness of  $\sim 35$ – $40 \text{ \AA}$ . Here, the deposition is terminated. These values of the conductance are chosen to be comparable to the conductance of the single molecules reported in the literature [4]. Note that the actual size of the junction can be much smaller than the tip diameter.

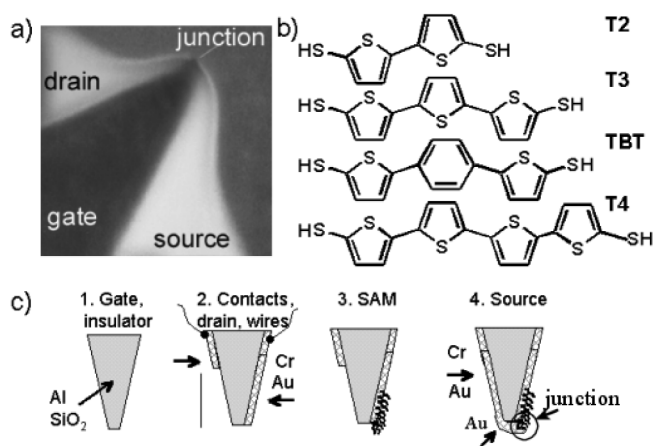


FIG. 1. (a) SEM image of the fabricated square tip. (b) Molecules used in the current work. (c) Sequence of the sample preparation: (1) metal gate (Al, 15 nm) and gate insulator ( $\text{SiO}_2$ , 50 nm) are deposited on the top face of the tip. (2) Contact pads are deposited  $\sim 10$  mm away from the tip end. The right face of the tip is covered with Cr (1 nm, adhesion promoter), Au (15 nm), forming the drain electrode. Electrical wires are attached. (3) A self-assembled monolayer is formed on the drain by dipping the tip into a solution with dithiol molecules. (4) The source electrode is formed in two steps: first, 15 nm Au is deposited from the left; second, Au is deposited from the tip side until the desired conductance is detected. The typical thickness of the last deposition is 3–4 nm.

The yield of good working devices is quite high, of the order of 80%–90%.

Under vacuum, the junctions are relatively stable in time, displaying some switching noise. The conductance decreases when the junctions are exposed to air. This phenomenon may be related to atomic diffusion at the metal surface, resulting in changes of the contact configuration at the metal-molecular interface. Having the thiol group at the top end of the molecule that covalently bonds to Au electrodes significantly improves the stability of the junctions. Still, we note that all the junctions change their electrical properties with exposure to air. Oxidation of the molecules or contamination of the junctions can also contribute to the conductance change. The change in the conductance varies with the molecule type: for shorter molecules (two thiophene rings) the conductance typically decreases from  $\sim 10^{-7} \Omega^{-1}$  to  $\sim 0.2\text{--}0.3 \times 10^{-7} \Omega^{-1}$ , while for longer molecules (four thiophene rings) the conductance degradation is down to  $\sim 5 \times 10^{-9} \Omega^{-1}$ .

The main experimental observation is demonstrated in Fig. 2. At low temperatures, all investigated samples display a set of distinct conductance steps periodic in source-drain bias ( $V_{sd}$ ). While the overall conductance curves vary noticeably for different samples, or for different cooling cycles of the same sample, the similar steplike features in conductance can be found in almost every sample and measurement of a particular molecule. The right inset of Fig. 2a shows the differential conductance measured on two different devices made of T3 molecules at 4.2 K, with the resonance peaks corresponding to the steps in the conductance. Although some deviations from the period-

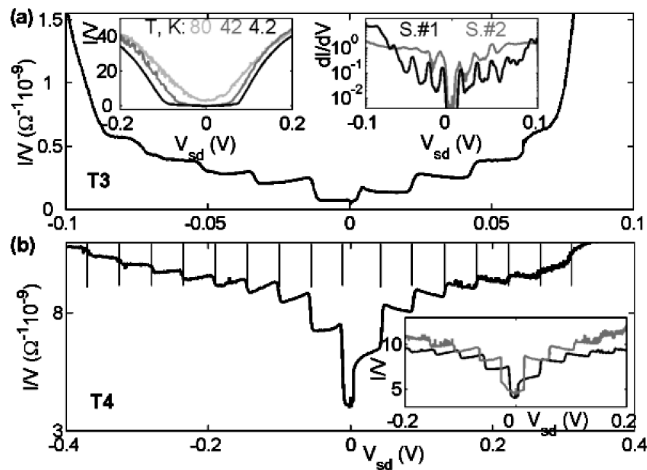


FIG. 2. (a) Conductance of the T3 sample as a function of source-drain bias at  $T = 4.2$  K. The steps in conductance are spaced by 22 mV. Left inset: conductance vs source-drain bias curves taken at different temperatures for the T3 sample (the room temperature curve is not shown because of large switching noise). Right inset: differential conductance vs source-drain bias measured for two different T3 samples at  $T = 4.2$  K. (b) Conductance of the T4 sample.  $T = 4.2$  K. Sixteen steps separated by 45 mV are seen. Inset: conductance curves for the T4 sample for two different cooling cycles. The conductance steps are shifted, but the spacing remains the same.

icity is seen, with some peaks doubling (dark curve) and switching (light curve), the main separation between the peaks is  $\sim 22$  mV for both samples. The conductance measurements for the T4 sample are shown in Fig. 2b for two different cooling cycles. The position of the conductance steps is shifted as a function of  $V_{sd}$  but the spacing remains the same. On some samples, the steps are very sharp with their width decreasing linearly as a function of temperature down to 0.3 K. At finite temperature, the steps broaden and eventually disappear at about  $\sim 100$  K. At room temperature the conductance is nearly independent of  $V_{sd}$ , displaying significant switching noise.

The step position as a function of  $V_{sd}$  can be affected by gate voltage. This is illustrated in Fig. 3, where families of conductance curves are plotted at different gate voltages ( $V_g$ ). This picture maps the dependence of the energy levels responsible for the conductance steps on both  $V_{sd}$  and  $V_g$ . The overall behavior is rather complicated at small biases ( $\sim 50$  mV around zero  $V_{sd}$  for Fig. 3a), but at higher biases there is a simple regularity. The most prominent feature is the periodic tilted stripe pattern. The edges of the stripes are the positions of the main steps. These edges often appear ragged (Fig. 3a) because of switching events. On average, every particular step shifts toward larger  $V_{sd}$  as  $V_g$  increases. The step position on the  $V_{sd} - V_g$  plane forms a curve consisting of straight segments with high slopes that are alternating with segments with either smaller (Fig. 3a) or negative (Fig. 3b) slopes. One possible reason for the deviation from linear dependence is an interaction of the main energy levels with other relevant energy levels in the molecular system. Another possibility is charging of traps in the insulator near the junction. Such charging effectively shifts the electrical potential seen by the molecules. For the T2 device (Fig. 3a),

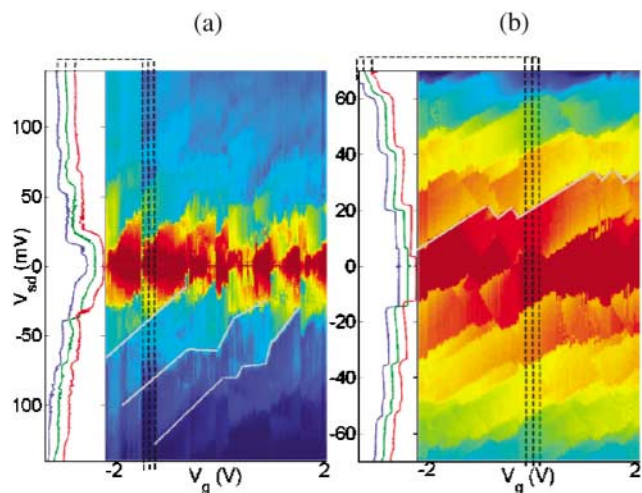


FIG. 3 (color). Conductance curves (coded with color) measured at different gate voltages. The left panels show three typical curves from the color diagram (the curves are shifted for clarity). (a) T2 sample.  $T = 4.2$  K. (b) T3 sample.  $T = 0.3$  K. The light lines are guides to the eyes showing the trajectory of the steps on  $V_{sd}$ - $V_g$  plane.

the main levels deviate from the linear dependence over a significant part of the picture, so that the steps are almost never exactly equidistant in  $V_{sd}$  at any particular  $V_g$ . Still, from Fig. 3a it can be determined that the preferred spacing is 38 mV. Similarly, for the T3 device (Fig. 3b) the spacing in every vertical cut is not strictly universal, with some splitting seen, but on average the value of 22 mV can be obtained.

Similar periodic behavior of the conductance steps is seen on all other samples. The step position depends linearly on the combination of  $V_{sd}$  and  $V_g$  with sample-specific factors. The deviations from linear dependence, such as crossing with other energy levels or step splitting, are not universal. The results for different molecules are summarized in Table I. Only the spacing for the main sequence of steps is listed. The spacing is reproducible within 5% on different samples for the first three molecules. The results for T4 molecules are less reproducible, with three main spacings found on different samples.

On all samples except the TBT molecules, it was possible to observe the steps near zero  $V_{sd}$ . An example of the typical low energy behavior is shown in Fig. 4. The amplitude of the step decreases as the step position is driven toward zero by adjusting  $V_g$ , and the step height is proportional to  $V_{sd}$  in the range of small biases. The step is followed by a change of slope in  $IV$  curves. Another reproducible family of features appearing as the change of slope in  $IV$  curves can be seen. The position of these kinks is shifted in the opposite direction in  $V_{sd}$  as a function of  $V_g$ . The lines marking the position of the two types of peculiarities on the  $V_{sd}$ - $V_g$  plane intersect at zero  $V_{sd}$  (inset of Fig. 4). Both features originate from the tunneling through the same molecular level, aligned with the Fermi level in either source or drain electrodes. The asymmetry is likely related to the different coupling strength of the source and the drain contact. The alignment is regulated by the electric potential. The gate potential coupling is 50–100 times less effective than the source-drain bias, consistent with the sample geometry. From the sign of the slope, the main steps are identified as a resonant alignment with the source. The fifth column in Table I lists the electrode association of the main sequence of the steps for different samples.

The periodic structure in conductance relates intuitively to the Coulomb blockade [12]. Indeed, many steps are seen in the conductance of small metal tunnel islands as a function of the source-drain voltage, and the overall behavior is

periodic as a function of gate voltage. The charging energy of the order of  $\sim 1$ –2 eV is expected for a single isolated molecule, although values as low as 0.2 eV have been used [5]. The spacing between the observed conductance steps is in tens of mV, which is typical for a metal island of 5–20 nm size. It is conceivable that such metal islands can form between the main electrode and the molecular junction. This scenario can be ruled out based on the reproducibility of the resonant structure on different samples for a given molecule. It is highly unlikely that the metal islands are of exactly the same size for a given molecule type and that the size varies with the molecule.

The fair reproducibility of the  $IV$  structure calls for assigning its origin to molecular properties. The appropriate energy is within the range of intramolecular vibrations. The reported lowest vibration modes are listed for thiophene oligomers in Table I [13]. These modes are in-plane, out-of-phase ring vibrations relative to the molecular center of mass. Such modes can be more relevant for the tunneling through the molecule than the higher-energy local modes associated with specific bonds. In inelastic electron tunneling spectroscopy, the vibrations are visible in the tunneling spectrum [14,15]. When the energy of an incident electron exceeds the energy of the vibration, energy transfer becomes possible and the tunneling probability is modified. Typically, the conductance change is no larger than a few percent [15]. The position of the inelastic feature is solely tied to the source-drain voltage difference.

We suggest that the conductance steps originate from the energy levels created by an electronic level coupled with an integer number of vibration quanta. The tunneling process is resonant, resulting in a significant conductance change. The electronic level can be somewhat below the Fermi level in Au ( $\sim 200$ –600 mV [5]). Resonant inelastic tunneling was proposed to describe tunneling through adsorbate molecules in scanning tunneling microscope experiments [16,17]. In our case, the electronic level is affected by the linear combination of the bias potential and the gate potential.

The steps are equally narrow at any gate voltage (Figs. 3 and 4). This means that only one molecule is electrically active. Otherwise, different capacitive couplings of different molecules to the gate electrode would result in the variation of the positions and width. The vibration mode that appears in the tunneling spectrum is the one that modifies the total tunnel barrier the most and/or strongly couples with the electronic level.

TABLE I. Conductance steps on different molecular junctions:  $V_{sd}$  spacing between the steps, maximal number of the steps seen for particular molecule, number of measured samples. The slope of the lines marking the steps on the  $V_{sd}$ - $V_g$  plane depends on which electrode the respective molecular level is in resonance. The last column lists the energies of the lowest molecular vibrations.

Molecule	Spacing (mV)	No. steps	No. samples	Slope	$E_{ph}$ (meV)
T2	38	10	3	Source	36
T3	22	8	4	Source	26
TBT	125	6	3	Drain	
T4	35, 45, 24	26, 18, 8	7	Varies	20

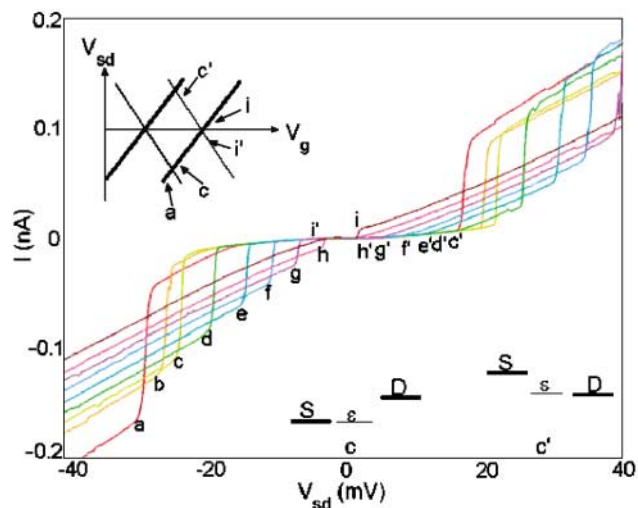


FIG. 4 (color). Series of  $IV$  curves showing the details of the resonances on the T4 sample near zero  $V_{sd}$ . The gate voltage ( $V_g$ ) varies from  $-0.85$  V (red curve) to  $+0.85$  V (brown curve). Two types of features are seen in the curves. The first type appears as a step in  $IV$  followed by a change of slope. Its position moves toward higher  $V_{sd}$  as  $V_g$  is increased (labeled with  $a, b, \dots, i$ ). The second type is seen as a change of slope moving toward lower  $V_{sd}$  as  $V_g$  is increased (labeled with  $c', d', \dots, i'$ ). Top inset: diagram illustrating the positions of the two types of features on the  $V_{sd}$ - $V_g$  plane. The thick lines are the step positions; the thin lines are the changes of slope. Bottom inset: the features can be identified as molecular level alignment with the Fermi level in source ( $c$ ) or drain ( $c'$ ) electrodes.

It has been recognized recently [18–20] that the coupling between a tunneling electron and molecular deformations enhances the tunneling probability in the gap region. However, it is rather surprising to observe the large number of resonances with slowly decreasing amplitude (Fig. 2b). This requires strong electron-vibration coupling. In optical spectroscopy of T2 and T4 molecules, only 3–4 vibration satellites are seen to accompany the electronic transition [13]. Apparently, the coupling in our case is strongly enhanced in comparison with optical experiments. The molecules are bonded to metal electrodes, and some charge is transferred to the molecule as the sulfur-gold bond is formed [21]. The tunneling process places an electron charge on the molecule, whereas during optical excitation the molecule remains neutral. We hope that a more complete theoretical treatment can clarify this problem.

Finally, little is known about the coupling between the molecules in the self-assembled monolayers. While the available experimental study implies that there is very small in-plane electronic overlap between the neighboring molecules [22], there are indications that the ordering of the conjugated oligomers in SAM is close to the packing of the bulk crystals [23]. The conduction bands in the molecular crystals are rather narrow, and the coherent band transport can be destroyed by temperature [24], disorder, or increased spacing. The possibility that the tunneling elec-

tron can be delocalized over the molecule-specific length within SAM cannot be ruled out. In this case, the delocalization length could be related to the polaron formation.

We acknowledge useful discussions with C. Varma, T. Fulton, B. Shraiman, K. Matveev, J. Moore, H. Hwang, R. de Picciotto, and G. Blumberg.

- [1] Z. J. Donhauser *et al.*, *Science* **292**, 2303 (2001).
- [2] X. D. Cui, A. Primak, X. Zarate, J. Tomfohr, O. F. Sankey, A. L. Moore, D. Gust, G. Harris, and S. M. Lindsay, *Science* **294**, 571 (2001).
- [3] S. Datta, W. Tian, S. Hong, R. Reifenberger, J. I. Henderson, and C. P. Kubiak, *Phys. Rev. Lett.* **79**, 2530 (1997).
- [4] M. A. Reed, C. Zhou, C. J. Muller, T. P. Burgin, and J. M. Tour, *Science* **278**, 252 (1997).
- [5] C. Kergueris, J. P. Bourgouin, S. Palacin, D. Esteve, C. Urbina, M. Magoga, and C. Joachim, *Phys. Rev. B* **59**, 12 505 (1999).
- [6] D. Porath, A. Bezryadin, S. deVries, and C. Dekker, *Nature (London)* **403**, 635 (2000).
- [7] H. Park, J. Park, A. K. L. Lim, E. H. Anderson, A. P. Alivisatos, and P. L. McEuen, *Nature (London)* **407**, 57 (2000).
- [8] J. Chen, M. A. Reed, A. M. Rawlett, and J. M. Tour, *Science* **286**, 1550 (1999).
- [9] J. H. Schön, H. Meng, and Z. Bao, *Nature (London)* **413**, 713 (2001).
- [10] C. P. Collier *et al.*, *Science* **289**, 1172 (2000).
- [11] M. J. Yoo, T. A. Fulton, H. F. Hess, R. L. Willet, L. N. Dunkelberger, R. J. Chichester, L. N. Pfeiffer, and K. W. West, *Science* **276**, 579 (1997).
- [12] H. Grabert and M. H. Devoret, *Single Charge Tunneling* (Plenum Press, New York, 1992).
- [13] D. Birnbaum and B. E. Kohler, *J. Chem. Phys.* **96**, 165 (1992).
- [14] R. C. Jaklevic and J. Lambe, *Phys. Rev. Lett.* **17**, 1139 (1968).
- [15] B. C. Stipe, M. A. Rezaei, and W. Ho, *Science* **280**, 1732 (1998).
- [16] B. N. J. Persson and A. Baratoff, *Phys. Rev. Lett.* **59**, 339 (1987).
- [17] M. A. Gata and P. R. Antoniewicz, *Phys. Rev. B* **47**, 13 797 (1993).
- [18] H. Ness, S. A. Shelvin, and A. J. Fisher, *Phys. Rev. B* **63**, 125422 (2001).
- [19] M. Olson, Y. Mao, T. Windus, M. Kemp, M. Ratner, N. Leon, and V. Mujica, *J. Phys. Chem. B* **102**, 941 (1998).
- [20] Z. G. Yu, D. L. Smith, A. Saxena, and A. R. Bishop, *Phys. Rev. B* **59**, 16001 (1999).
- [21] Y. Xue, S. Datta, and M. A. Ratner, *J. Chem. Phys.* **115**, 4292 (2001).
- [22] T. Ishida, W. Mizutani, U. Akiba, K. Umemura, A. Inoue, N. Choi, M. Fujihira, and H. Tokumoto, *J. Phys. Chem. B* **103**, 1686 (1999).
- [23] S. Frey, V. Stadler, K. Heister, W. Eck, M. Zharnikov, M. Grunze, B. Zeysing, and A. Terfort, *Langmuir* **17**, 2408 (2001).
- [24] J. Schön, C. Kloc, and B. Batlogg, *Phys. Rev. Lett.* **86**, 3843 (2001).